Lunar Radii Determined from Lunar Orbiter 1 V/H Sensor Data

WILLIAM R. WELLS*
University of Cincinnati, Cincinnati, Ohio

Introduction

THE Lunar Orbiter series of satellites revealed the potential use of orbiting satellites to gather various types of physical data on a celestial body. Among these data types are surface photography and gravitational field characteristics. In the case of the Lunar Orbiter satellites, another data type was discovered which provided a means of determining the lunar equatorial radius. This data was in the form of an extremely accurate angular velocity reading from an electro-optical device known as the image-motion compensator sensor (V/H sensor) used to stabilize the film during the open period of the shutter of the photographic system. The function of this sensor was to provide a mechanical shaft rotation, proportional to the image motion, to drive the camera platen through a cam and lever arrangement. The ideal result of the platen motion is to completely stabilize the film during the entire time the system shutter is open. The output of the system was divided by the focal length of the camera lens. This ratio was then telemetered back to Earth as a V/H measurement. The V/H measurement together with the spacecraft state vector are used to determine the local lunar radius at the point of measurement.

Operation of V/H Sensor

In general, operation of the V/H sensor was initiated just prior to photographing a given site. The selenographic latitude and longitude of the desired photo site were predetermined and shortly before a picture-taking sequence the camera optical axis was aligned along a direction parallel to the local vertical of the desired photo site. The V/H sensor was then put into operation and used to control the camera platen speed throughout the photographing sequence.

The V/H sensor on the Lunar Orbiter spacecraft scanned the lunar surface through a portion of the 24 in. camera lens outside the normal image format. A small rectangular aperture, located on a scanner disk, rotated in a circle at the rate of 4000 rpm or one scan every 0.015 sec. During one scan or one rotation of the rectangular aperture, an annulus with outer radius of approximately 1.6 km and inner radius of about 1.3 km is swept out on the surface of the moon. Between successive rotations of the scanner disk, the lunar scene necessarily changes due to the motion of the spacecraft. The V/H sensor detects the shift in the image and attempts to null the image shift by changing the camera-platen speed. (See Fig. 1 which was taken from Ref. 1.)

The V/H tracking cycle is defined by the motion of the tracking optics over a fixed time interval during which the angle θ (Fig. 2) between the camera optical axis and the V/H axis varies from about 10° to 6°. However, the exact value of this angle at any given time is not known. For the purpose of this analysis, an average value of 8° was assumed. At the end of each tracking cycle, the V/H axis was reset to a position 10° ahead of the optical axis and a new tracking cycle was begun.

The basic sensor consists of a lens system that creates an image on the surface of the scanner, which in turn examines the image and generates an electrical signal that uniquely

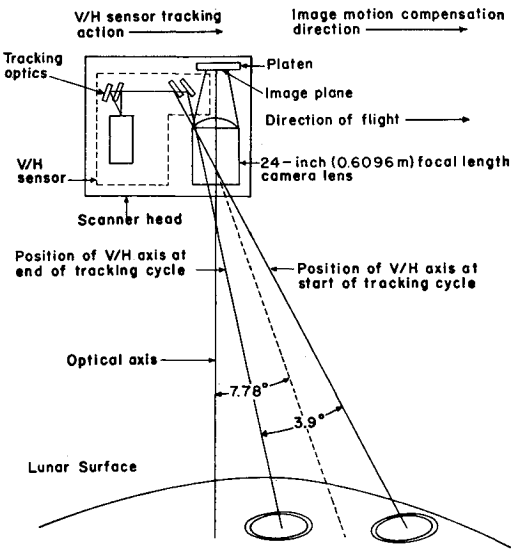

Fig. 1 V/H sensor operation.

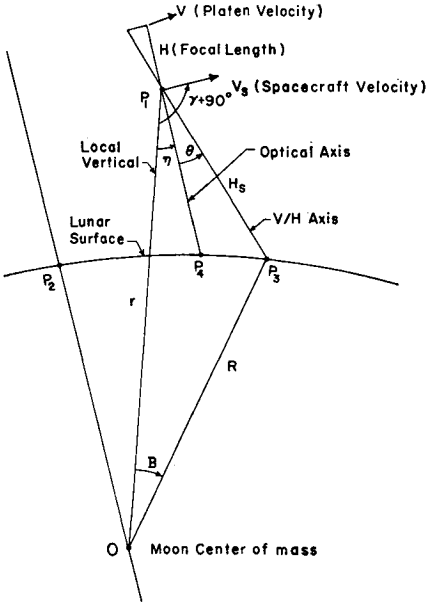

Fig. 2 Spacecraft-lunar-surface photography.

defines the examined image. At the beginning of a cycle, the line of sight (V/H axis) is swung forward to about 10°. The image viewed at this position is scanned and the electrical signal generated is memorized. As the satellite passes over the terrain, a closed-loop servo maintains the system line of sight point at the memorized area of the terrain; thus the image on the face of the scanner stays constant and unchanged to the extent that the system gain and response time are able to provide perfect image stabilization. Further details of the V/H sensor can be found in Refs. 1 and 3.

Lunar Radius Calculation

The relationship of the V/H reading to the lunar radius can be determined from Fig. 2. The position of the spacecraft at the time of orientation of the optical axis along the local vertical of the photo site is P_1. The photo site is at point P_2. The point on the lunar surface being scanned by the V/H sensor is P_3. Line P_1P_4 is parallel to the local vertical at point P_2. The angle η is the tilt angle defined as the angle

Received September 7, 1971, revision received February 18, 1972.
Index categories: Unmanned Lunar and Interplanetary Systems; Data Sensing and Preparation or Transmission Systems.

* Associate Professor, Department of Aerospace Engineering, University of Cincinnati. Associate Fellow AIAA.

between the local vertical and the optical axis. The tilt angle is positive whenever the optical axis leads the local vertical. The time history of this angle was obtained from photo support data from Ref. 4.

The V/H value is obtained by dividing the platen velocity, V, by the focal length, H. The platen velocity is

$$V = d/(\mathrm{H}\ \tan\theta)/dt = \dot{\theta}H/\cos^2\theta \tag{1}$$

From Fig. 2 $\dot{\theta}$ is determined to be

$$\dot{\theta} = (V_s/H_s)\cos(\theta + \eta - \gamma) \tag{2}$$

where V_s is the magnitude of the spacecraft velocity vectors, H_s is the straight line distance along the V/H axis to point P_3 on the lunar surface, and γ is the flight path angle.

From Eqs. (1–2) the V/H value is determined as

$$\mathrm{V/H} = V_s\cos(\theta + \eta - \gamma)/H_s\cos^2\theta \tag{3}$$

The value for V_s was obtained from an orbit determination program while γ is computed from the two-body relation

$$\tan\gamma = e\ \sin v/(1 + e\ \cos v) \tag{4}$$

The eccentricity e and true anomaly v were obtained from an orbit determination program.

The lunar radius R is determined from consideration of triangle P_1OP_3 in Fig. 2 as

$$R = [r^2 + H_s^2 - 2rH_s\cos(\theta + \eta)]^{1/2} \tag{5}$$

where r, the magnitude of the position vector of the spacecraft, is obtained from the orbit determination program. Substitution for H_s from Eq. (3) into Eq. (5) results in

$$R = \left[r^2 - \frac{2rV_s\cos(\theta + \eta - \gamma)\cos(\theta + \eta)}{(V/H)\cos^2\theta} + \frac{V_s^2\cos^2(\theta + \eta - \gamma)}{(V/H)^2\cos^4\theta}\right]^{1/2} \tag{6}$$

The selenographic latitude ϕ and longitude λ corresponding to the radius of Eq. (6) are determined from

$$\begin{aligned}
\sin\phi &= \sin i\ \sin(\omega + v + \beta)\\
\sin\gamma\ \cos\phi &= \cos(\omega + v + \beta)\ \sin\Omega + \cos i\ \cos\Omega\ \sin(\omega + v + \beta)\\
\cos\lambda\ \cos\phi &= \cos(\omega + v + \beta)\ \cos\Omega - \cos i\ \sin\Omega\ \sin(\omega + v + \beta)
\end{aligned} \tag{7}$$

The angles i, ω, and Ω are the inclination, argument of periapse and longitude of ascending node of the orbit. These angles are illustrated in Fig. 3 and are determined from the orbit determination program. The angle β is calculated from the equation

$$\beta = \sin^{-1}[(H_s/R)\sin(\theta + \eta)] \tag{8}$$

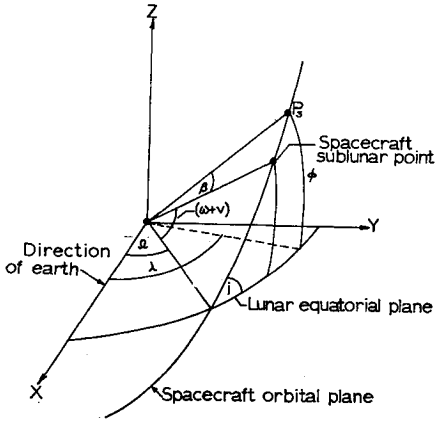

Fig. 3 Orbital plane relative to a selenographic coordinate system.

Error Analysis

In order to obtain an estimate of possible radii error, three error sources were considered: the uncertainty in the determination of the spacecraft radius, the uncertainty in the angle θ, and the biases associated with the V/H sensor. The sensor was designed to operate between 8 and 50 mrad/sec and in fact operated well within this design during the Lunar Orbiter I flight. Also, there has been no evidence from the lunar photographs to indicate that the sensor operated improperly. The maximum uncertainty in θ and the spacecraft radius has been estimated to be $\pm 2°$ and ± 0.5 km, respectively. By assuming the maximum uncertainty in these two parameters, and assuming that the spacecraft radius error is entirely along the lunar radius, the estimated possible error in the magnitude of the lunar radius is ± 0.7 km.

The selenographic coordinates of the lunar radii locations have errors associated with them due to the uncertainty in the angle θ, the uncertainty of the V/H sample point within the scanning annulus, and the uncertainty in the orientation of the spacecraft radius vector. The maximum error in the angle θ leads to a possible error of 1.7 km in the location of P_3 on the lunar surface. The V/H sample was assumed to have been at the center of the scanning annulus although it was somewhere between the outer and inner circle. This assumption leads to a possible error of 1.6 km in the location of P_3 on the lunar surface. Finally, the orientation of the spacecraft radius vector was assumed to be in error by 0.095° of arc at the center of the moon. This assumption corresponds to about a 3 km error at the spacecraft in the position vector and to a possible error of 2.7 km in the location of P_3. By adding the three errors in the location of P_3, a possible maximum error of 6 km or 0.2° central angle is obtained.

Two additional error sources which were assumed to be negligible should be mentioned. These are the error introduced by neglecting the velocity of the lunar surface at point P_3 and the error introduced in the V/H value due to possible perturbations in the angular velocity from limit cycle motion of the vehicle about the desired attitude.

Discussion of Results

The primary result presented in this paper is the determination of the lunar radii in the vicinity of the equatorial region of the moon. These radii are plotted in Fig. 4 as a function of longitude. The maximum latitude for either of these radii is 2.2° north and 4.0° south. The maximum lunar radius of 1738.6 km occurs in the mountainous region just to the east of the Central Bay (Sinus Medii) area. The minimum lunar radius of 1734.6 km occurs in Mare Tranquillitatis. The arithmetic mean of the lunar radii is 1736.5 km or about 1.5 km smaller than the mission planning value of 1738.09 km. From Fig. 4 an asymmetrical bulge toward the Earth in the Central Bay area of the lunar equator can be seen. This same type of bulge was observed in the results in Ref. 5.

A comparison of the results of this paper with those obtained from other techniques is given in Fig. 4. The solid curve in Fig. 4 represents the results for lunar radius variations in the

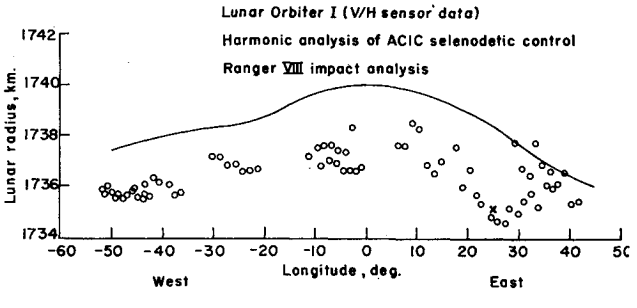

Fig. 4 Comparison of lunar orbiter I results with other analyses.

Table I Comparison of Lunar Orbiter I values of lunar radius with radar and photogrammetric values

Lunar Orbiter				Radar			
Latitude, deg	Longitude, deg	Radius, km	Accuracy, km	Latitude, deg	Longitude, deg	Radius, km	Accuracy, km
−2.86	−6.71	1737.70	±0.7	−2.95	−6.72	1737.17	±0.3
−3.15	−5.28	1737.50		−2.27	−5.96	1737.36	
1.05	−5.74	1737.00		1.17	−5.27	1737.21	
0.73	−4.33	1736.76		0.70	−4.51	1737.34	
Lunar Orbiter				Photogrammetric			
0.37	34.08	1735.35	±0.7	0.37	34.08	1734.82	±0.2
0.07	35.49	1736.20		0.07	35.49	1735.82	
−0.23	36.91	1736.09		−0.23	36.91	1735.60	
0.11	−1.51	1736.77		0.11	−0.15	1736.13	
−3.23	−36.14	1735.88		−3.23	−36.14	1735.31	
−2.08	−43.81	1735.60		−2.08	−43.81	1735.31	
−2.37	−42.39	1735.76		−2.37	−42.39	1735.26	
−2.35	−44.47	1735.67		−2.35	−44.47	1735.65	
−2.64	−43.06	1735.74		−2.64	−43.06	1735.42	

equatorial region from a harmonic analysis by Bray and Goudas of a selenodetic control system of the U.S. Air Force Aeronautical Chart and Information Center (ACIC) (Ref. 5). These results, derived from Earth-based photography, are with respect to the center of figure of the moon. The Lunar Orbiter values are smaller on the average by about 2 km. Some agreement is seen in the region from 30° to 40° east longitude. Note the appearance of an asymmetrical bulge in the solid curve similar to that previously mentioned for the Lunar Orbiter results. Also shown in Fig. 4 is a radius determination with respect to the center of mass of the moon from Ranger VIII impact analysis. (See Ref. 7.) This value is in agreement with Lunar Orbiter values. The trends illustrated in Fig. 4 indicate that the radii relative to the center mass of the moon are systematically less than those relative to the center of figure which suggests a displacement of the center of mass of the moon toward the Earth, relative to the center of figure.

A comparison of Lunar Orbiter I values with recent radar and photogrammetric determinations is presented in Table I. The radar values were taken from Ref. 5 and were chosen to coincide as closely as possible to the Lunar Orbiter points. The few radar points which are compared are in agreement and appear to support the Lunar Orbiter I data. The photogrammetric data (Ref. 8) are lower than the Lunar Orbiter I data. The differences, which range from 0.2 km to about 0.6 km, lie well within the respective accuracies of the values presented.

Conclusions

The lunar radius has been determined in the equatorial region from about 50° west to 40° east selenographic longitude. The lunar radius was found to be about 2 km smaller, on the average, than the accepted value prior to the Ranger VIII and the Lunar Orbiter flights. The suggestion of an asymmetrical bulge toward the earth was noted in the general area of Sinus Medii. Comparisons of the Lunar Orbiter I values of the radii were made with those determined from a harmonic analysis, Ranger VIII impact analysis, radar measurements, and photogrammetric technique. In general, the Lunar Orbiter I values agree with these results with the exception of the harmonic analysis. The radii presented in this paper lie within a band ±4° of the lunar equator and no limb data has been included. In order to substantiate the lower mean value presented in this report, it would be helpful to include data over the entire interval from the western to the eastern limb. Since the radii presented in this report are with reference to the center of mass of the moon, a displacement of the center of mass of the moon toward the earth, relative to the center of figure is suggested.

References

[1] Photographic Subsystem Reference Handbook for the Lunar Orbiter Program, L-018375-RU, March 1966, Eastman Kodak Co., Rochester, N.Y.

[2] *Evaluation of Motion-Degraded Images*, NASA SP-193, Washington, D.C., 1968.

[3] Compton, Harold R., and Wells, William R., "Determination of Lunar Equatorial Radius Using Image-Motion Compensation Sensor Data From Lunar Orbiter I," TN-D-5231, June 1969, NASA.

[4] "Lunar Orbiter I—Postmission Photo Supporting Data," CR-66481, 1967, NASA.

[5] Shapiro, A., Uliana, E. A., Yaplee, B. S., and Knowles, S. H., "Lunar Radius From Radar Measurements," *Proceedings of the International Space Science Symposium—7th—Vienna—1967. Moon and Planets Two: A Session of the Joint Open Meeting of Working Groups One, Two, and Five of the Tenth Planetary Meeting of COSPAR*, edited by A. Dollfus. North Holland Publishing Co., Amsterdam, Holland, 1968, pp. 34–46.

[6] Bray, T. A., and Goudas, C. L., "A Contour Map Based on the Selenodetic Control System of A.C.I.C.," *Icarus*, Vol. 5, No. 5, 1966, pp. 526–535.

[7] Sjogren, William J., Trask, Donald W., Vegos, Charles J., and Wollenhaupt, Wilbur R., "Physical Constants as Determined From Radio Tracking of the Ranger Lunar Probes," *Proceedings of the Space Flight Mechanics Specialist Symposium*, American Astronautical Society, Vol. 11, 1967, pp. 137–154.

[8] Jones, Ruben L., "An Analytical Study of Lunar Surface Shape and Size From Lunar Orbiter Mission I Photographs," TN-D-5243, 1969, NASA.